Generic Torque-Maximizing Design Methodology of Surface Permanent-Magnet Vernier Machine

Akio Toba, *Member, IEEE*, and Thomas A. Lipo, *Fellow, IEEE*

***Abstract*—A surface permanent-magnet vernier machine (SPMVM) has a toothed-pole structure, and its highly nonlinear relationship between its dimensions and magnetic field makes its design cumbersome. This paper presents a generic design methodology for the machine which brings out its torque-maximizing structure in a convenient manner. Various suggestions concerning the design of the SPMVM are also set forth.**

***Index Terms*—Case study, design, experiment, permanent magnet, theoretical analysis, torque, vernier machine.**

I. Introduction

A SURFACE permanent-magnet vernier machine (SPMVM) has the desirable feature of high torque at low speed and, therefore, is regarded as a suitable alternative for direct-drive applications such as robot arms or electric vehicles [1]–[4]. The high torque feature is brought about by the so-called "magnetic gearing effect," which is based on its toothed-pole structure. In this structure, the relationship between the dimensions and the magnetic flux distribution becomes significantly nonlinear, and this feature makes design optimization a time-consuming process requiring a repetition of numerical field analyses such as finite-element method (FEM). This paper presents a novel generic design methodology for the SPMVM, which realizes a torque-maximizing structure in a convenient manner. The following are the main topics of this paper:

1) introduction of a general torque equation for the SPMVM, which gives insight into the theory of its torque production and a clear reason for the choice of the magnet pole number;
2) introduction of a basic building block of the SPMVM, the elementary domain (ED) [3], for a simple but rational means for torque prediction;
3) magnetic field analyses of the ED with FEM, and an elaborate arrangement of the results to a generic form;
4) proposal of a convenient design procedure based on the above items and confirmations of its validity by a case study and an experiment.

Paper IPCSD 00–038, presented at the 1999 IEEE International Electric Machines and Drives Conference, Seattle, WA, May 9–12, and approved for publication in the IEEE TRANSACTIONS ON INDUSTRY APPLICATIONS by the Electric Machines Committee of the IEEE Industry Applications Society. Manuscript submitted for review July 2, 1999 and released for publication June 29, 2000.

A. Toba is with Fuji Electric Corporate Research and Development, Ltd., Tokyo 191-8502, Japan (e-mail; akio-toba@fujielectric.co.jp).

T. A. Lipo is with the Department of Electrical and Computer Engineering, University of Wisconsin, Madison, WI 53706-1691 (e-mail: lipo@engr.wisc.edu).

Publisher Item Identifier S 0093-9994(00)10419-0.

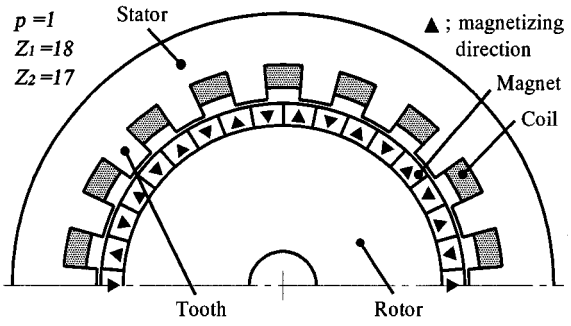

Fig. 1. SPMVM.

II. Generic Torque Analysis of SPMVM

Fig. 1 shows the half-cross-sectional view of a typical three-phase SPMVM. The stator has a toothed-pole structure, which has windings in slots with a conventional overlapped configuration, and the rotor has surface permanent-magnet poles. The stator and the rotor are constructed by steel laminations. In this machine, there exists the following rule:

$$Z_2 = Z_1 + p \quad \text{or} \quad Z_1 - p \tag{1}$$

where p, Z_1, and Z_2 are the numbers of winding pole pairs, stator teeth, and rotor pole pairs, respectively.

Due to this rule, a unique phenomenon appears, as to be explained with Fig. 2. This figure shows the difference of the flux distribution with the rotor position in an SPMVM. The parameters of the machine are $p = 1$, $Z_1 = 18$, and $Z_2 = 17$. The flux is due only to the permanent magnet, and between Fig. 2(a) and (b), there is a slight difference of the rotor positions, which corresponds to a quarter of the stator tooth pitch. It is noted that the number of the pole pairs of the flux distribution equals the value of p. Thus, a steady torque is yielded by synchronizing the coil magnetomotive force (MMF) to the flux rotation. It is also observable that the flux distribution changes 90 electrical degrees with the indicated difference of the rotor position. That is, a small movement of the rotor makes a large change of the flux, which results in a high torque. This phenomenon based on the rule (1) is called the "magnetic gearing effect."

A general torque equation of the SPMVM can be obtained thorough the analysis of the flux density and the MMF in the air gap. The following are the assumptions for the analysis.

- The magnetic resistance and saturation of the steel parts are neglected.
- The relative permeability of the permanent magnet is unity, the same as the air. The part consists of the air gap and the permanent magnet is named a "virtual air gap."

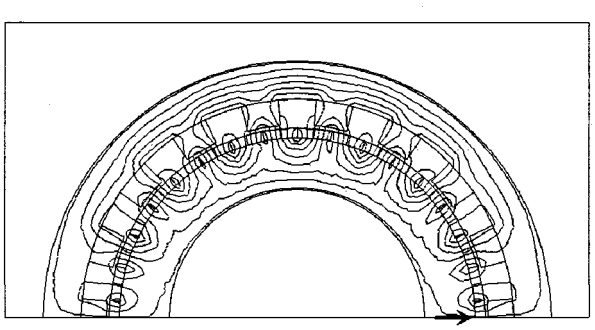

(a)

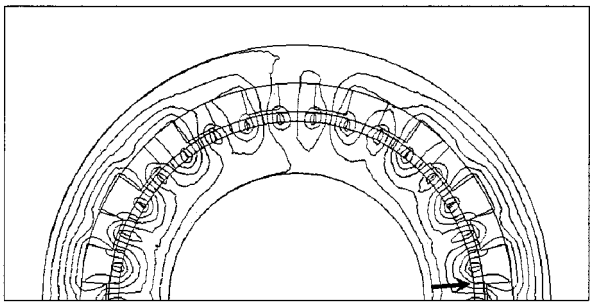

(b)

Fig. 2. Change of the flux distribution in an SPMVM with rotor position (no coil current). (a) Rotor position *A*. (b) Rotor position *B*.

- The flux density, MMF, and permeance in the air gap vary only with the circumference direction and are uniform with the radial and the axial direction.
- The three-phase balanced sinusoidal current $i_x (x = \mathrm{U, V, W})$ is assumed for the coil excitation, expressed as

$$i_x = \sqrt{2} I \cos\left(\omega t - \alpha + \frac{2\pi}{3} a\right), \tag{2}$$

where $I$is the effective value of i_x, ω is the angular frequency of the coil current, $a$is an arbitrary angle, and $a = 0$, 1, and 2 for the phases U, V, and W, respectively.

The MMF of the permanent magnet can be expressed as

$$\begin{aligned} F_{PM}(\theta_1) &= \sum_{n;\mathrm{odd}}^{\infty} \frac{F_{PM1}}{n} \cos(n Z_2 \theta_2) \\ &= \sum_{n;\mathrm{odd}}^{\infty} \frac{F_{PM1}}{n} \cos\{n Z_2 (\theta_1 - \theta_m)\} \end{aligned} \tag{3}$$

where F_{PM1} is the amplitude of the fundamental component of F_{PM}, and θ_1, θ_2, and θ_m are the mechanical angle on the stator, the one on the rotor, and the rotor position, respectively, the details of which are shown in Fig. 3. The angle $\theta_1 = 0$ is the direction of the positive coil current vector of phase U, $\theta_2 = 0$ is the center of a particular magnet pole which is magnetized to the air gap, and $\theta_m = \theta_1 - \theta_2$. Because of the toothed-pole structure, the permeance per unit area to the radial direction in the air gap, which is called the *permeance coefficient P* in this paper, can be expressed as

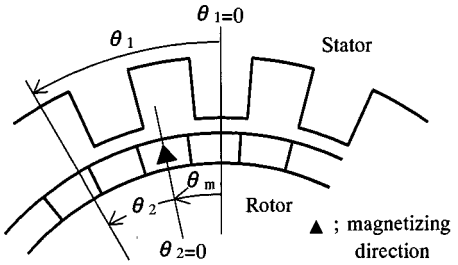

Fig. 3. Definition of mechanical angles.

$$P(\theta_1) = P_0 + (-1)^j \sum_{m=1}^{\infty} P_m \cos(m Z_1 \theta_1) \tag{4}$$

where P_m is the amplitude of the permeance coefficient of the mth harmonic, and j is the number of slot shifts for the short pitch windings ($j = 0$; full-pitch). The air-gap flux density due to the permanent magnet is the product of F_{PM} and P. Hence, concerning only the major terms of F_{PM} and P, i.e., $n = 1$ and $m = 1$, and neglecting the higher order component than Z_2, the air-gap flux density due to the permanent magnet, B_{PM}, is obtained as

$$\begin{aligned} B_{PM} &\approx [F_{PM1} \cos\{Z_2(\theta_1 - \theta_m)\}] \left[P_0 + (-1)^j P_1 \cos(Z_1 \theta_1)\right] \\ &\approx (-1)^j B_{PM1} \cos\{(Z_2 - Z_1)\theta_1 - Z_2 \theta_m\} \\ &\quad + B_{PMh} \cos\{Z_2(\theta_1 - \theta_m)\} \end{aligned} \tag{5}$$

where

$$B_{PM1} = \frac{F_{PM1} P_1}{2} \quad \text{and} \quad B_{PMh} = F_{PM1} P_0. \tag{6}$$

Here, the right-most side of (5) is investigated in detail. It is noted that the first term component has the same spatial period to the fundamental component of the coil MMF because of (1). It is also realized with referring to (1) that the spatial period of the second term component is the same to that of one of the slot harmonics of the coil MMF, since the orders of the slot harmonics are $Z_1/p \pm 1$. Moreover, the rotational directions of the first and second terms are the same if Z_2 is chosen to $Z_1 + p$, while they become opposite to each other when Z_2 is set to $Z_1 - p$. In general, the higher and the lower order components of the slot harmonics of the coil MMF rotate to the same and the opposite directions with the fundamental component, respectively. Hence, if the fundamental component of the coil MMF is synchronous to the first term component of B_{PM}, as is usually the case, the second term component of B_{PM} also becomes synchronous to its corresponding slot harmonic component of the coil MMF and, thus, the interaction of these two harmonic components yields a steady torque, not a ripple torque. This interaction is called the *harmonic coupling* in this paper.

The harmonic coupling and its effect on the net torque in the PMVM are suggested in the pioneering works by the groups of Ishizaki [1], [2] and Llibre [3]. The machine in [1] and [2] is slightly different from the SPMVM, while [3] deals with the same machine as this paper. In any case, the relationship of (1) is maintained and the torque production is based on the same prin-

ciple described herein. Nevertheless, there is a need for more detailed analysis of this phenomenon, because [1] and [2] concentrate on the case of $Z_2 = Z_1 + p$, and [3] deals only with the amplitudes of the harmonics. To investigate the torque, however, the phases of the harmonics must be taken into account, which has not yet attracted much attention. The phases of the harmonics can be proven to make a critical difference in the torque production between the cases of $Z_2 = Z_1 - p$ and $Z_2 = Z_1 + p$, as will be shown below.

The air-gap MMF due to the coil current, F_c, is expressed as follows, which takes account of the phases of the harmonics:

$$F_c(\theta_1, t) = \frac{3F_{c1}}{2}\left[\sum_{n=1,7,13,\cdots}\frac{k_{dn}k_{pn}}{n}\cos\{np\theta_1-(\omega t-\alpha)\} + \sum_{n=5,11,17,\cdots}\frac{k_{dn}k_{pn}}{n}\cos\{np\theta_1+(\omega t-\alpha)\}\right] \tag{7}$$

where

$$F_{c1} = \frac{2\sqrt{2}NI}{p\pi} \tag{8}$$

and N is the total number of turns of the windings per phase. The quantities k_{dn} and k_{pn} are the distribution factor and the pitch factor of the nth harmonic, respectively, which are defined as follows:

$$k_{dn} = \frac{\sin(n\pi/6)}{q\sin(n\pi/6q)} \tag{9}$$

$$k_{pn} = \sin(n\beta\pi/2) \tag{10}$$

where q is the number of slots per pole per phase, and β is the ratio of the coil pitch to the winding-pole pitch. Among β, j, and q, there is the following relationship:

$$\beta = 1 - (j/3q). \tag{11}$$

Here, care must be taken due to the fact that k_{pn} must be calculated even for the full-pitch winding ($\beta = 1$), to take the phases of the harmonics into account. For example, substituting $\beta = 1$ and $n = 7$ into (10) makes $k_{p7} = -1$, and this affects the polarity of the seventh harmonic. The only concern with the components of F_c here is terms having the same orders as the terms in B_{PM}, since otherwise they do not affect net torque. Thus, taking only the fundamental and the slot harmonics, one obtains

$$F_c \approx \frac{3k_{d1}k_{p1}F_{c1}}{2}\left[\cos\{p\theta_1-(\omega t-\alpha)\} + \frac{(-1)^j}{Z_1/p-1}\cos\{(Z_1-p)\theta_1+(\omega t-\alpha)\} + \frac{(-1)^{j-1}}{Z_1/p+1}\cos\{(Z_1+p)\theta_1-(\omega t-\alpha)\}\right]. \tag{12}$$

If all the field energy is regarded to be stored in the air gap and the permanent magnet (the virtual air gap), which is usually adequate, the net torque T can be calculated as

$$T = \frac{p\lambda l}{\pi}\int_0^{2\pi}\left\{\frac{\partial}{\partial\theta_m}\left(\frac{1}{2}BF\right)\right\}d\theta_1 = \frac{p\lambda l}{\pi}\int_0^{2\pi}\left\{P(F_c+F_{PM})\frac{\partial F_{PM}}{\partial\theta_m}\right\}d\theta_1 \tag{13}$$

where

- λ winding-pole pitch;
- l stack length of the steel;
- B, F flux density and the MMF in the virtual air gap, respectively.

From (3) to (6) and (12) and (13), it works out to

$$T = \frac{3}{2}p\lambda l Z_2 k_{d1}k_{p1}F_{c1}\left(B_{PM1} \mp \frac{B_{PMh}}{Z_2/p}\right)\cdot\sin\{(\omega t-\alpha) \mp Z_2\theta_m\} \tag{14}$$

where the orders of the dual signs in (14) agree with the order of $Z_2 = Z_1 \pm p$, and the number of slots per pole per phase q is an integer. From (5) and (6), B_{PM1} and B_{PMh} correspond to the fundamental and the slot harmonic components, respectively. Hence, it is revealed that the harmonic coupling increases the net torque when $Z_2 = Z_1 - p$, and decreases it when $Z_2 = Z_1 + p$. Since B_{PMh} becomes much higher than B_{PM1}, the torque due to the harmonic coupling has a great impact on the net torque [1]–[3]. Consequently, the choice of Z_2 should be $Z_1 - p$ for the higher torque production, with employing an integer number of q (the number of slots per pole per phase) to maximize the slot harmonics of the coil MMF.

It is also clear that the steady torque is obtained by setting

$$\omega = \pm Z_2\omega_m \tag{15}$$

where $\theta_m = \omega_m t$, ω_m is the angular frequency of the rotor rotation, the order of the dual sign is the same as $Z_2 = Z_1 \pm p$, and the maximum torque comes out when $\alpha = \pm\pi/2$. Substituting these parameters into (14) gives the expression of the maximum steady torque T_m as

$$T_m = 3\sqrt{2}\frac{\lambda l}{\pi}Z_2 k_{d1}k_{p1}NI\left(B_{PM1} \mp \frac{B_{PMh}}{Z_2/p}\right). \tag{16}$$

III. Elementary Domain

A. Concept of the Proposed Methodology

Although a general expression of the torque of the SPMVM has been obtained, significant nonlinearities in the actual field are not reflected in the analysis in the previous section. Therefore, for reasonable calculations of the torque, the numerical field analysis should be employed. Because the aim of this research is to establish a generic method of the torque-maximizing design, it is desirable to break the torque expression into some basic factors, which can be linearly recombined, and to analyze these factors including nonlinearities. This is explained here, starting with the study of the flux distribution due to the permanent magnet in a flattened vernier structure shown in Fig. 4. The figure shows only a quarter of a vernier structure, for which

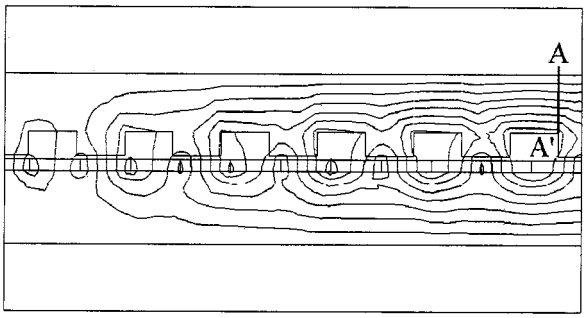

Fig. 4. Flux distribution in a Vernier structure.

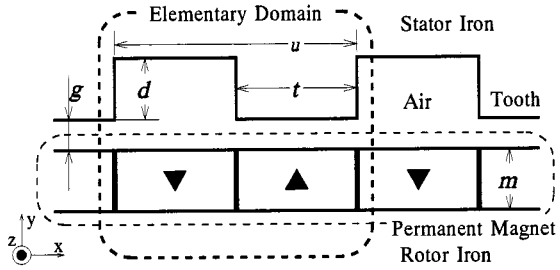

Fig. 5. ED.

$Z_1 = 24$ and $Z_2 = 23$, and the symmetrical flux distribution is assumed for the rest of the structure. The magnet pole is aligned to the tooth at the left side, while it is unaligned at the right side. In this placement of the magnet poles, the conductor in the right-most slot experiences the maximum flux linkage, and the major part of this flux crosses the line segment A–A'. In an actual machine, this flux is equivalent to half of the maximum flux due to the permanent magnet which links to a full-pitch concentrated winding Φ. Φ can be regarded as being composed of two factors; the sum of all the flux passing through the teeth, and the flux circulating around only the right-most slot. The former corresponds to the fundamental component Φ_1 and the latter corresponds to the slot harmonic component Φ_h. equation (16) can be rewritten with these fluxes as

$$T = \frac{3}{\sqrt{2}} Z_2 k_{d1} k_{p1} NI(\Phi_1 + 2\Phi_h) \tag{17}$$

where $\Phi = \Phi_1 + 2\Phi_h$. From the comparison of (16) and (17), it is noted that there are the following relationships:

$$\Phi_1 = \frac{2}{\pi} \lambda l B_{PM1} \tag{18}$$

$$\Phi_h = \frac{2}{\pi} \frac{\lambda l}{Z_2/(2p)} B_{PMh}. \tag{19}$$

These equations indicate that Φ_1 and Φ_h are the integrals of sinusoidal waves whose amplitudes are B_{PM1} and B_{PMh}, respectively, over one positive half waveform.

In (17), T is proportional to Z_2, which makes the SPMVM a high-torque-at-low-speed-type machine. On the other hand, T is also proportional to Φ, which will decrease monotonically with Z_2 because of the leakage flux among adjacent permanent-magnet poles. Hence, in terms of pursuing the maximum torque, there is a tradeoff between Z_2 and Φ.

In (17), all the parameters except Φ can be clearly specified. Therefore, by quantifying the relationship between the structural dimensions and Φ, the torque can be calculated. To implement this in a general form, an ED will be introduced.

B. ED

The SPMVM is considered to have a basic building block consisting of one tooth, one slot, and one magnet pole pair. This building block is defined as an "*ED*" in [3]. Fig. 5 shows the ED, with the dimensions specifying the structure, which are: g, air-gap length; m, magnet thickness; d, slot length; and u, tooth pitch. In the ED, the tooth pitch and the magnet-pole pitch are the same. The ED is a two-dimensional structure and uniform with the z direction in the figure. The widths of tooth and slot can be different but are set to be equal here for convenience.

C. Reflection of ED to the Torque Expression

1) Fundamental Component: One can define Φ_S as the amplitude of the total magnetic flux passing normally to the tooth pitch of one ED when the tooth and magnet are aligned. The flux Φ_S can be expressed as (20), which also defines an "*effective-flux coefficient* k_F"

$$\Phi_s = ulk_F B_r \tag{20}$$

where l is the z-direction thickness of the ED, and B_r is the remanence of the magnet. In an SPMVM, magnetic flux that passes normally to the teeth contributes to the torque production. Hence, k_F shows the effectiveness of the structure to exploit the potential of the magnet. Lining up the EDs in the x direction and short circuiting the upper and lower yoke magnetically results in an *ED array*. In an ED array, the same magnetic field distribution is assumed for each ED. If the number of the EDs in one array is n, the total effective flux Φ_T becomes

$$\Phi_T = n\Phi_s = nulk_F B_r. \tag{21}$$

In an actual SPMVM, the number of teeth in a full-pitch coil is $Z_1/(2p)$. In this case, Φ can be expressed as (22), taking account of the effect that the numbers of teeth and magnet pole pairs in one coil pitch are different because of (1)

$$\Phi_1 = V \frac{Z_1}{2p} ulk_F B_r \tag{22}$$

where V is defined as a "*vernier coefficient*," which represents the effect just described.

2) Slot Harmonic Component: The flux in the ED corresponding to the slot harmonic can be obtained from the model in Fig. 6. In this model, the magnet poles are unaligned to the tooth, and the field values on the left and right boundaries are set equal to each other. Since the concerning flux can either circulate around the slot or flow through the two boundaries, the net flux passing the line segment A–A' in the figure, Φ_h, should be the required one. It is possible to express Φ_h in a similar way to Φ_S, which is

$$\Phi_h = ulk_{Fh} B_r \tag{23}$$

where k_{Fh} is an "*effective-flux coefficient of the slot harmonic*."

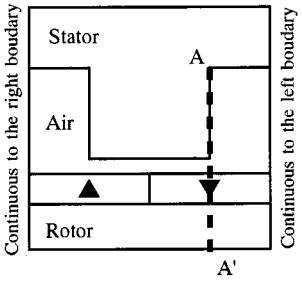

Fig. 6. ED with unaligned magnet poles.

3) Torque Expression: Substituting (22) and (23) into (17) yields

$$T_m = \frac{3}{\sqrt{2}} Z_2 k_{d1} k_{p1} NI \left(V \frac{Z_1}{2p} k_F + 2k_{Fh} \right) uB_r = \frac{3}{\sqrt{2}} ulZ_2 \frac{\pi R}{p} k_{d1} k_{p1} NIB_r \left(V \frac{k_F}{u} + \frac{2p}{\pi R} k_{Fh} \right) \quad (24)$$

where R is the radius of the air gap, the circumference of which is uZ_1. Usually, Z_1 is selected more than ten times as large as p. Thus, it is a good approximation to assume $Z_1 \approx Z_2$ based on (1), whereupon

$$T_m = 3\sqrt{2} \frac{(\pi R)^2 l}{p} k_{d1} k_{p1} NIB_r \left(V \frac{k_F}{u} + \frac{2p}{\pi R} k_{Fh} \right). \quad (25)$$

IV. FEM Analysis of Elementary Domain

A. Preparations

Field analyses of the ED have been done by the Maxwell 2D Field Simulator, Version 6.5.04 (Ansoft Company). From the preliminary analyses, several important facts were uncovered.

1) The smaller the value of g is, the larger k_F and k_{Fh} become.
2) Similar but different size EDs show the same k_F and k_{Fh}, i.e., it is sufficient to analyze the ED with setting one parameter among g, m, d, and u to be constant. The air-gap length g is the most suitable for the fixed parameter. The other parameters can now be normalized by g as

$$m' = m/g \quad d' = d/g \quad u' = u/g \quad R' = R/g. \quad (26)$$

It is also preferable to modify the torque equation (25) with the normalized parameters as

$$T_m = 3\sqrt{2} \frac{(\pi R)^2 l}{pg} k_{d1} k_{p1} NIB_r \left(V \frac{k_F}{u'} + \frac{2p}{\pi R'} k_{Fh} \right). \quad (27)$$

In this equation, only the inside of the last parentheses depends on the toothed-pole structure. Hence, it can be used as a torque-maximizing index with the toothed-pole dimensions as parameters. Therefore, the *torque-maximizing index* k_T can be defined as

$$k_T = V \frac{k_F}{u'} + \frac{2p}{\pi R'} k_{Fh}. \quad (28)$$

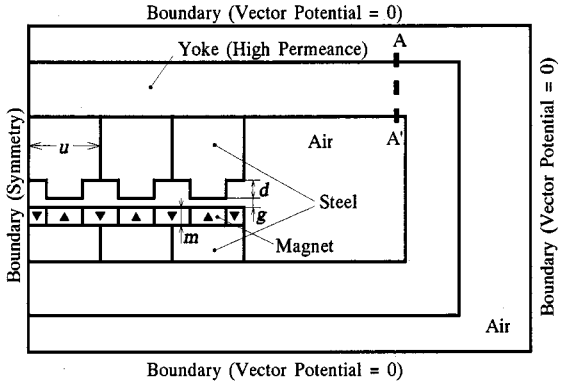

Fig. 7. Analyzed model of an ED array.

TABLE I
Material Settings of the Analyzed Model

Magnet	Br=1.23T, Hc=-8.9×10^{5}A/m (NdFeB)
Steel	μ_r=2200, saturation over about 1.5T
Yoke	μ_r=10^7, linear property

B. Investigation of k_F

Fig. 7 shows the ED array utilized for an investigation of k_F. Therein, three EDs and an adjacent symmetry boundary result in six EDs. Table I shows the material settings of the model. By assigning a high permeance to the yoke, magnetic field distribution of each ED becomes the same. The value k_F is obtained from the flux passing through the line segment A–A' (Φ_a) by using

$$k_F = \frac{\Phi_a}{3ulB_r}. \quad (29)$$

Fig. 8 shows some examples of k_F-to-u' curves with various values of m' and d'. Ranges of the parameters have been chosen over practical values. From the acquired curves, the following facts are revealed.

1) In the practical range, the maximum value of k_F is about 0.25.
2) With constant m' and u', k_F for $d' = 0.4u'$ is over 98% of k_F for $d' = 0.5u'$ in all cases. Hence, setting $d' = 0.4u'$ is sufficient from the torque increase point of view.

Fig. 9 shows k_F/u'-to-u' curves with various values of m' and d'. The following points are perceived from the curves.

1) There exists a k_F/u' maximizing u' in each case, and it increases as m' increases.
2) The selection of u' becomes critical when m' is small because of the steep slope of the k_F/u'-to-u' curve.

C. Investigation of k_{Fh}

The investigation of k_{Fh} is implemented with the model shown in Fig. 6. Fig. 10 exhibits some of the k_{Fh}-to-u' curves. From the curves, the following facts can be mentioned.

1) There is a peak in each of the curves.
2) In the practical range, the maximum value of k_{Fh} is about 0.1.

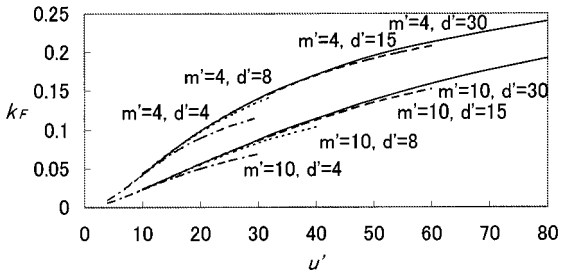

Fig. 8. k_F-to-u' curves.

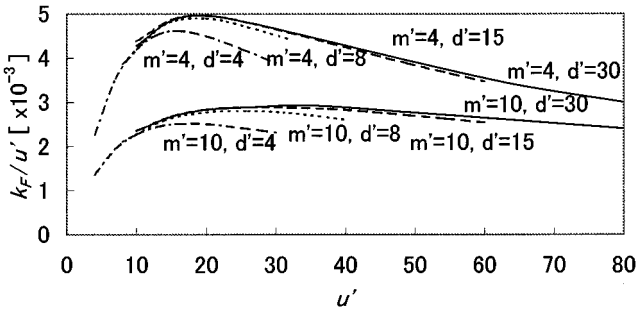

Fig. 9. k_F/u'-to-u' curves.

3) The greater the value m', the greater becomes the quantity k_{Fh}.
4) With constant m' and u', the values of k_{Fh} for $d' = 0.4u'$ and $d' = 0.5u'$ are almost the same in any case. Thus, setting $d' = 0.4u'$ is sufficient in terms of increasing torque.

D. Investigation of V

Fig. 11 shows the model analyzed to investigate the value of V, which is the same structure shown in Fig. 4. As is described in Section III-A, there is the following relationship with the flux passing through the line segment A–A', Φ_v:

$$\Phi_v = \frac{1}{2}\Phi = \frac{1}{2}(\Phi_1 + 2\Phi_h). \tag{30}$$

Substituting (22) and (23) into (30) and arranging it by using the relationship $\lambda = uZ_1/(2p)$, one can obtain the expression of V as

$$V = \frac{2}{l\lambda k_F B_r}(\Phi_v - ulk_{Fh}B_r). \tag{31}$$

The values of k_F and k_{Fh} are obtained from the curves acquired above.

Fig. 12 shows some examples of the relationship between V and Z_1 with various values of m and λ. It is noted that the variation of V is fairly small with the parameters chosen, as well as over the practical ranges of the parameters. Therefore, to establish an efficient design procedure, V is fixed to near the average value, 0.55.

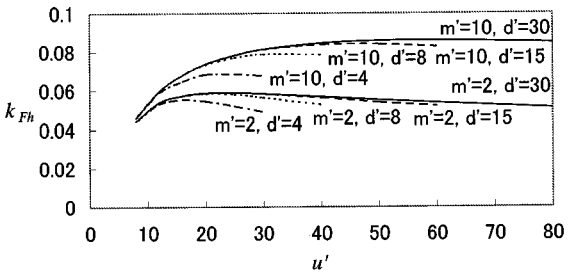

Fig. 10. $k_{Fh} - u'$ curves.

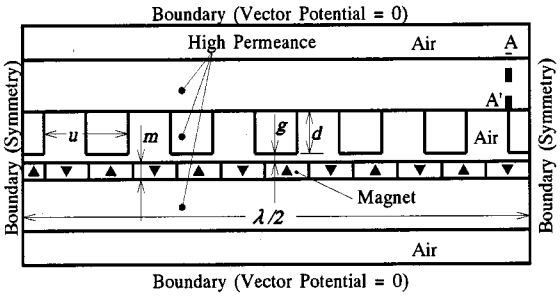

Fig. 11. Analyzed model for the investigation of V.

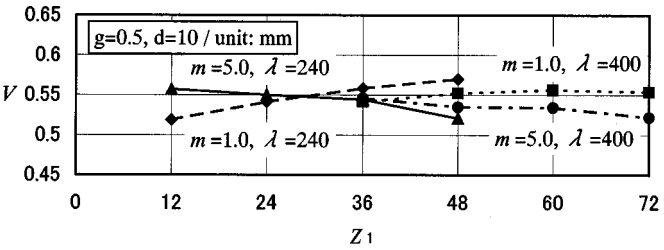

Fig. 12. V-to-Z_1 curves.

V. Proposal and Evaluations of Design Methodology

A. Design Procedure

Based on the preceding discussion, the torque-maximizing design of an SPMVM can be achieved through a simple procedure as follows.

1) Set the initial condition (machine diameter, stator inner radius, air-gap length, coil specifications, magnet material, etc.)
2) Set the magnet thickness from the condition to avoid the irreversible demagnetization of the permanent magnet by the coil excitation.
3) Set the slot length temporarily, acquire the k_T-to-u' curve, and identify the torque-maximizing $u'(u'_m)$. Check the slot length being appropriate compared to an index, $d = 0.4u$.
4) Choose Z_1 as an integer so that the tooth pitch becomes the closest to the torque-maximizing value. Set Z_2 to $Z_1 - p$.

The procedure is suitable for being implemented as a computer program with a data base for k_F and k_{Fh}, which makes the design optimization quite easy.

TABLE II
CONDITIONS OF THE CASE STUDY

Stator	R=44, l=60, g=0.4, outer radius; 60 [mm]
Magnet	Br=1.23T, Hc=-8.9×10^{5}A/m
Coil	p=1, I=4.4A(max. 8.8A), N=100turn

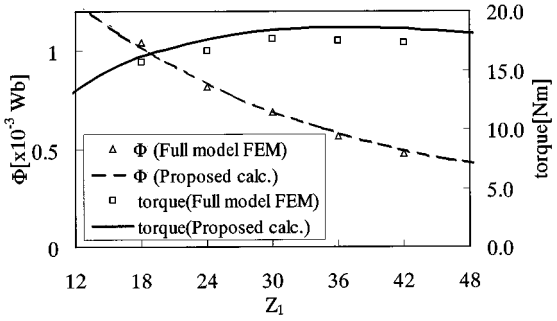

Fig. 13. Result of the case study.

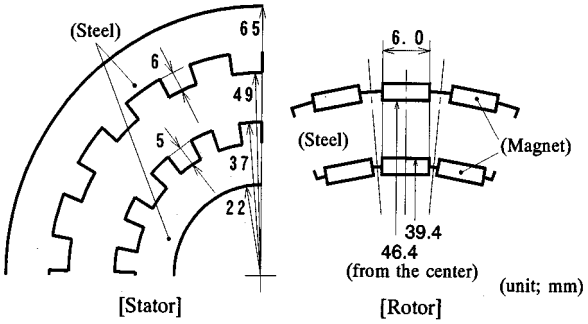

Fig. 14. Major dimensions of the prototype DEPMVM.

B. Case Study

To check the validity of the proposed method, a case study has been carried out. Table II lists the conditions of the case study. The magnet thickness is set to 1.6 mm from the coil specifications, and the slot length d is chosen as 6 mm, i.e., $m' = 4.0$ and $d' = 15.0$. In this case, u'_m is about 20 and, thus, the slot length is sufficiently large. Therefore, the parameters can be determined as follows: $Z_1 = 30$, $Z_2 = 29$, $u = 2\pi R/Z_1 = 9.2$ mm, and $d = 6$ mm.

Fig. 13 shows the flux Φ and the torque with various values of Z_1 in the SPMVM for the case study. Both values of the flux and the torque are acquired from each of FEM analyses with full machine models and the calculations presented in this paper. The calculated values agree very well with the FEM-based ones, and it is noted that the torque becomes a maximum around $Z_1 = 30$.

C. Experimental Study of a Prototype Machine

A prototype machine of the SPMVM type has been fabricated and tested [4]. Fig. 14 shows the structure and dimensions of the machine, and Table III summarizes the major specifications. This machine has a special feature, which is that the rotor is ring shaped and two stators exist inside and outside the rotor.

TABLE III
SPECIFICATIONS OF THE PROTOTYPE DEPMVM

Z_1=18, Z_2=17, p=1, Slots/pole/phase/stator; 3
Number of coil turns; 26 (outer), 18 (inner) /slot
Rated current; 4.4A, Rated speed; 300r/min
Rated power; 530W, Rated torque; 16.9Nm
Permanent Magnet; NdFeB(Br=1.23T, Hc= -8.9×10^5 A/m)
thickness; 2.0mm
Steel lamination stack length; 60mm

TABLE IV
COIL-INDUCED VOLTAGES OF THE PROTOTYPE

Voltage(phase)	Analysis	Experiment
Outer stator	27.7Vrms	27.3Vrms
Inner stator	14.5Vrms	15.3Vrms

The torque due to the inner and the outer structures is regarded to be independent, as long as the steel is not magnetically saturated. By generator tests, the no-load induced voltages are obtained, which are proportional to the available torques to be evaluated in case the magnetic saturation in the steel is negligible. Table IV shows the analytical and experimental values of the induced voltage with no load, rated speed rotation. Good agreement is observed with both of the stators, which supports the validity of the proposed method.

VI. CONCLUSIONS

A novel torque-maximizing design methodology for the SPMVM has been presented through quantitative analyses of the machine. Compared to the conventional method, the design policy is clear, and the design effort is greatly reduced in the proposed method. Some important suggestions for the design of the SPMVM have also been provided.

REFERENCES

[1] A. Ishizaki, *et al.*, "heory and optimum design of PM vernier motor," in *Proc. IEE Int. Conf. Electrical Machines and Drives '95*, 1995, pp. 208–212.
[2] A. Ishizaki, *et al.*, "Study on optimum design of PM vernier motor" (in Japanese), *Trans. Inst. Elect. Eng. Jpn.*, vol. 114-D, no. 12, pp. 1228–1234, 1994.
[3] J.-F. Llibre and D. Matt, "Harmonic study of the effort in the vernier reluctance magnet machine," in *Proc. ICEM'98*, 1998, pp. 1664–1669.
[4] A. Toba and T. A. Lipo, "Novel dual-excitation permanent magnet vernier machine," in *Conf. Rec. IEEE-IAS Annu. Meeting*, 1999, pp. 2539–2544.

Akio Toba (S'93–M'94) is a native of Tokyo, Japan. He received the B.E. and M.E. degrees in electrical engineering from Tokyo Metropolitan University, Tokyo, Japan, in 1992 and 1994, respectively.

Since 1994, he has been with Fuji Electric Corporate Research and Development, Ltd., Tokyo, Japan. From 1997 to 1999, he was a Visiting Scholar in the Department of Electrical and Computer Engineering, University of Wisconsin, Madison. His research interests include electric machines, ac drives, and power electronics.

Thomas A. Lipo (M'64–SM'71–F'87) is a native of Milwaukee, WI. From 1969 to 1979, he was an Electrical Engineer in the Power Electronics Laboratory, Corporate Research and Development, General Electric Company, Schenectady NY. He became a Professor of electrical engineering at Purdue University, West Lafayette, IN, in 1979 and, in 1981, he joined the University of Wisconsin, Madison, in the same capacity, where he is presently the W. W. Grainger Professor for power electronics and electrical machines.

Dr. Lipo has received the Outstanding Achievement Award from the IEEE Industry Applications Society, the William E. Newell Award of the IEEE Power Electronics Society, and the 1995 Nicola Tesla IEEE Field Award from the IEEE Power Engineering Society for his work. Over the past 30 years, he has served the IEEE in numerous capacities, including President of the IEEE Industry Applications Society.